# Measurement of Crack Opening Displacement and Energy Release Rate of Rapidly Bifurcating Cracks in PMMA by High-Speed Holographic Microscopy*

Shinichi SUZUKI** and Kenichi SAKAUE**

High-speed holographic microscopy is applied to take three successive photographs of fast propagating cracks at the moment of bifurcation. The cracks are propagated in PMMA plate specimens at a speed about 660 m/s. From the photographs, crack opening displacement (COD) is measured along the cracks as a function of distance $r$ from the crack tips. The measurement results show that the CODs are proportional to $\sqrt{r}$ before bifurcation. After bifurcation, the CODs of mother cracks are proportional to $\sqrt{r}$, however, the CODs of branch cracks are not always proportional to $\sqrt{r}$. Crack speed is also measured from the photographs. As a result, discontinuous change of crack speed is not observed at the moment of bifurcation. The energy release rate and energy flux toward crack tips are obtained from the COD data, and are found to be continuous across the bifurcation point. The energy release rate and energy flux increase gradually across the bifurcation point.

***Key Words***: Fracture Mechanics, Brittle Fracture, Crack Opening Displacement, Energy Release Rate, Crack Bifurcation, Optical Measurement, Holography, High-Speed Photography, Microscopy

## 1. Introduction

When brittle materials break under external force, there appear fast propagating cracks that are of opening mode and whose speed is from 200 to 2 000 m/s. When the crack speed is high enough, a fast propagating crack bifurcates into two cracks suddenly. Bifurcation is a characteristic feature of fast propagating cracks, accordingly, many researchers have studied it theoretically and experimentally[(1)-(12)]. But the mechanism of the rapid crack bifurcation has not been fully understood.

After bifurcation, the area of the crack surfaces that are newly made by the crack extension of unit length is twice as large as that before bifurcation. Consequently, if the crack speed after bifurcation is the same as that before bifurcation, the energy release rate of the crack after bifurcation must be twice as large as that before bifurcation. In order to understand the mechanism of rapid crack bifurcation it is important to make clear whether the discontinuous increase of the energy release rate really occurs or not. But this has been left as an open problem so far.

To answer the question, it is necessary to measure the energy release rate just before and after bifurcation. But it is very difficult to measure energy release rate just after bifurcation, because the two crack tips exist very close, thus strong interaction occurs between them. Hence there was no method to measure the energy release rate just after bifurcation.

Recently, high-speed holographic microscopy was applied to photograph fast propagating cracks at bifurcation[(10)-(12)]. The high-speed holographic microscopy has spatial resolution much higher than the other optical measurement method used in dynamic fracture research[(10)-(16)]. The stress field near bifurcating crack tips was measured accurately by the high-speed holographic microscopy with interferometry[(11)].

Utilizing the high spatial resolution of the high-speed holographic microscopy, the present study takes microscopic photographs of rapidly bifurcating cracks and measures crack opening displacement, COD, of the cracks just before and just after bifurcation. Crack speed is also measured from the photographs. Energy release rate and energy flux toward crack tips are obtained from the measured COD data.

* Received 5th January, 2004 (No. 04-4001)

** Department of Mechanical Engineering, Toyohashi University of Technology, 1–1 Hibarigaoka, Tempaku-cho, Toyohashi, Aichi 441–8580, Japan.
E-mail: shinichi@mech.tut.ac.jp

## 2. Experimental Method

### 2.1 Specimen

Figure 1 shows the transparent PMMA specimen used in the present study. It is 300 mm wide, 50 mm long and 3 mm thick, and has no notch. Uniform tensile stress is applied to the specimen, and a small defect is made by a knife-edge at the mid point A of the upper boundary of the specimen. A fast propagating crack arises from the defect and propagates toward the observation area at the center of the specimen. When propagating in the observation area, the crack bifurcates into two cracks. The crack speed at bifurcation is approximately 660 m/sec.

### 2.2 High-speed holographic microscopy[10]-[16]

When a specimen of brittle material breaks rapidly, the specimen surfaces vibrate. Consequently, it is impossible to focus a conventional microscope on a surface of the specimen during the rapid fracture phenomena. High-speed holographic microscopy can solve the problem and makes it possible to take microscopic photographs of fast propagating cracks.

**2.2.1 Holographic recording of cracks** Figure 2 (a) shows the optical system to record three successive holograms of a fast propagating crack. The optical system has three pulsed ruby lasers as light sources. A crack propagates in the PMMA specimen SP perpendicularly to the paper plane. When the crack is propagating in the observation area, the ruby lasers oscillate in the order of PL1, PL2 and PL3. The three laser beams record the crack as the first, the second and the third hologram, respectively. Laser pulse duration is approximately 30 ns, and the time between each laser oscillation and the next is about 5 μs.

The light beam emitted from pulsed ruby laser PL1 is divided into two parts by beam splitter BS1. The reflected light beam from BS1 is diverged by lens L1 and collimated by concave mirror CM. The collimated beam is reflected by mirrors M1 and M2, and falls upon holographic plate HP at the angle of incidence of 30 degrees. This is the reference beam for the first hologram.

The light beam transmitted through beam splitter BS1 is diverged by lens L4, reflected by mirror M7, and passes through beam splitters BS4 and BS5. Passing through lenses L7 and L8, the light beam becomes a parallel light beam. The parallel light bean passes through beam splitter BS6 and falls upon the specimen surface perpendicularly. The light beam is reflected either by surface SA or by surface SB of the specimen as shown in Fig. 2 (b). The reflected light from the specimen is reflected by beam splitter BS6, passes through imaging lens IL and impinges on the holographic plate perpendicularly. This is the object beam for the first hologram. The object beam makes real image RI of the crack and the specimen in front of holographic plate HP. Thus the optical system in Fig. 2 is of image plane holography.

The pulsed ruby lasers, PL2 and PL3, oscillate about 5 μs and 10 μs after the oscillation of PL1. Then the rapidly bifurcating crack is recorded as the second and third hologram on the same holographic plate. The angles of incidence of the three reference beams are different one

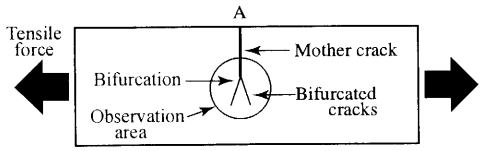


Fig. 1 PMMA plate specimen

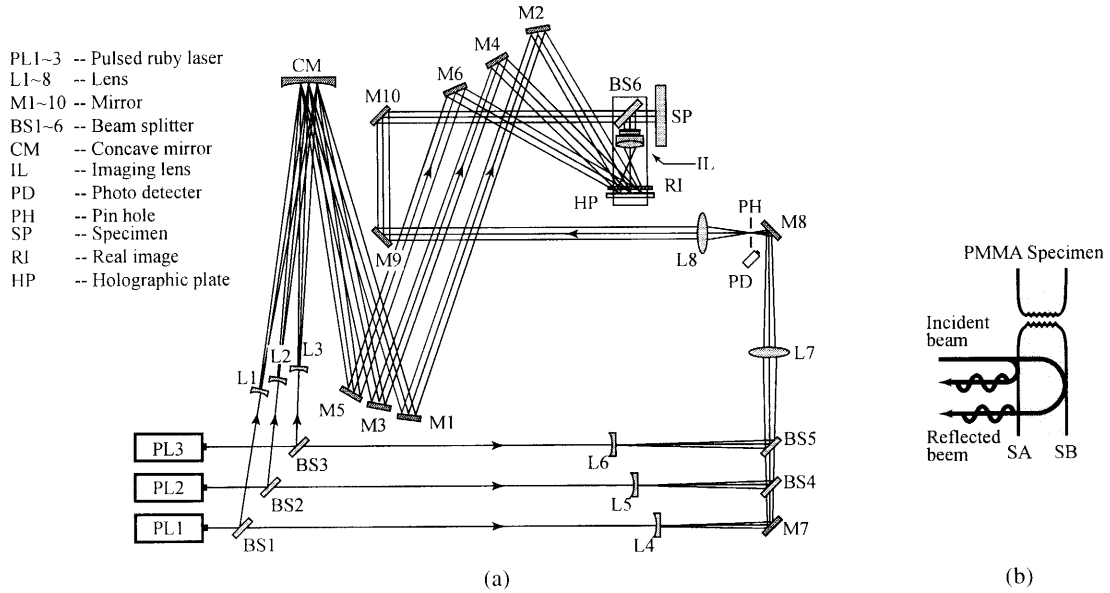


Fig. 2 Holographic recoding system for rapidly bifurcating cracks

another, 30, 45 and 60 degrees, then the three holograms have different carrier wave frequencies. This is the angle-multiplexing holography.

Photo detector PD measures the laser light and gives the time interval of $\tau_{i,i+1}$ between the $i$-th frame and the next.

**2.2.2 Reconstruction and microscopic photographing** Figure 3 shows the reconstruction and microscopic photographing of the crack images from the superimposed holograms. After developed, the holographic plate is placed at the same position as that of the recording, and is illuminated with a reconstruction beam that is a parallel beam of a He-Ne laser. The angle of incidence $\phi_i'$ of the reconstruction beam is given by the following equation[17],

$$\sin\phi_i' = (\lambda_H/\lambda_R)\sin\phi_i \quad (i=1,\ 2 \text{ or } 3) \qquad (1)$$

where $\phi_i$ is the angle of incidence of the reference beam for the $i$-th hologram, and $\lambda_H$ and $\lambda_R$ are the wavelengths of He-Ne lasers (633 nm) and ruby lasers (694 nm), respectively.

Reconstruction from the first hologram is shown in Fig. 3 (a). Illuminated with the reconstruction beam of the angle of incidence of $\phi_1'$, the first hologram reconstructs the conjugate beam of the first object beam. The conjugate beam propagates along the same optical path that the object beam propagated, but in the opposite direction. The conjugate beam passes through the imaging lens, is reflected by the beam splitter, and makes a real image of the crack at the position where it existed at the recording of the hologram. The real image of the crack is magnified and photographed through a conventional microscope. The microscope is focused on surface SA of the specimen in Fig. 2 (b), hence, the crack on surface SA is photographed.

When the holographic plate is illuminated with the reconstruction beam for the first hologram, the second and the third hologram emit light beams that correspond to the second and the third object beam. However, the light beams from the second and the third holograms are blocked up by the spatial filters in front of the imaging lens. The real image of the crack of the first hologram is therefore reconstructed separately.

The reconstruction from the second or the third hologram is carried out in the same manner as that from the first hologram as shown in Fig. 3 (b) and (c). The spatial resolution of the reconstructed images is more than 180 lines/mm, and the observation area is about 20 mm in diameter.

### 2.3 Measurement of Crack Opening Displacement (COD)

Crack opening displacements are measured along cracks on the photographs magnified by about 70 times. Figure 4 (a) shows COD measurement of the crack before bifurcation. The COD is measured along the crack as a function of distance $r$ from the crack tip. Figure 4 (b) shows the method to measure CODs of branch cracks. The COD of each branch crack is measured along it as a function of the distance $r$ from the tip of the branch crack. It is known that the lengths of branch cracks are approximately equal to one another.

Figure 4 (c) shows the method to measure the COD of the mother crack after bifurcation. Before measuring COD, one needs to define the position of the nominal tip of the mother crack. The present study defines the position of the nominal tip of the mother crack as follows.

( 1 ) The nominal tip of a mother crack is on the $x$-axis

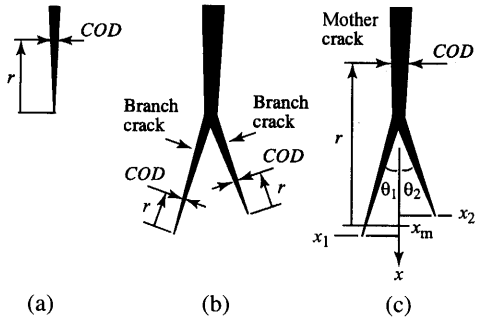


Fig. 4 Measurement of crack opening displacement

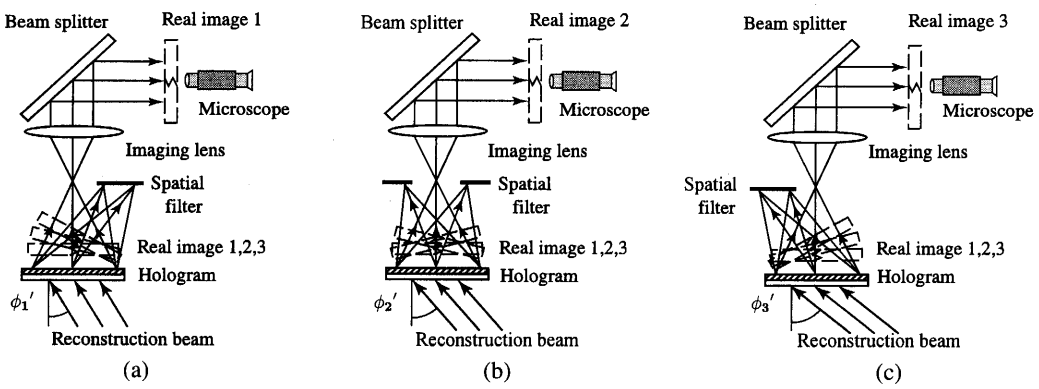


Fig. 3 Reconstruction and microscopic photographing of crack images

that is along the mother crack.

(2) The $x$-position, $x_m$, of the nominal tip is given by the equation,

$$x_m = \frac{1}{N}\sum_{i=1}^{N} x_i \tag{2}$$

where $x_i$ is the $x$-position of the $i$-th branch of the bifurcated crack, and $N$ is the number of branch cracks. The $x$-position, $x_i$, of each branch crack is nearly equal to those of the others, consequently, the value of $x_m$ is very close to that of every $x_i$. The crack opening displacement of a mother crack is measured as a function of the distance $r$ from the nominal tip determined by the above procedure.

### 2.4 Crack speed measurement

The crack speed before and after bifurcation is obtained from the three successive photographs. Figure 5 shows the method to measure the crack speed of a bifurcating crack. In Fig. 5 (a), the crack bifurcates between the first and the second frame. Extension lengths of the crack, $a_1$, $a_2$ and $a_3$, in $x$-direction are measured from the photographs, where $a_2$ and $a_3$ are determined from the position of the nominal tip of the mother crack. The frame interval $\tau_1$ and $\tau_2$ are also measured by the signal of the photo detector in Fig. 2. It is assumed that the crack speed is constant before and after bifurcation, respectively. Thus the crack speed $v_1$ before bifurcation and the crack speed $v_2$ after bifurcation in $x$-direction are obtained through the following equations,

$$(a_1/v_1)+(a_2/v_2)=\tau_1, \quad a_3/v_2=\tau_2. \tag{3}$$

If the bifurcation angle is small, the $x$-direction crack speed $v_2$ after bifurcation is approximately equal to the speed of branch cracks. Assuming that bifurcation occurs at the time of $t = 0$, the time of photographing of every frame, $t_1$, $t_2$ and $t_3$, is also obtained from the crack speeds $v_1$ and $v_2$, by the following equations.

$$t_1=-a_1/v_1, \quad t_2=a_2/v_2, \quad t_3=(a_2+a_3)/v_2 \tag{4}$$

In the case of cracks that bifurcate between the second and the third frames, Fig. 5 (b), crack speeds, $v_1$ and $v_2$, before and after bifurcation are obtained by the following equation,

$$a_1/v_1=\tau_1, \quad (a_2/v_1)+(a_3/v_2)=\tau_2, \tag{5}$$

and, the time of photographing of each frame is also obtained as follows,

$$t_1=-(a_1+a_2)/v_1, \quad t_2=-a_2/v_1, \quad t_3=a_3/v_2. \tag{6}$$

In the case of symmetric bifurcation, $\theta_1 = \theta_2 = \theta$ in Fig. 4 (c), the crack speed of a branch crack $v_b$ is given by following equation,

$$v_b=v_2/\cos\theta \tag{7}$$

### 2.5 Energy release rate and energy flux

#### 2.5.1 Energy release rate before bifurcation

The theory of dynamic fracture mechanics says that the COD of a fast propagating crack is proportional to $\sqrt{r}$. Hence, by measuring COD, it is possible to obtain the energy release rate $G(v)$ of the crack through the following formula of dynamic fracture mechanics[18],

$$\begin{aligned} G(v) &= \frac{1}{\mu}A_1(v)K_I^2 \\ K_I(v) &= \sqrt{\frac{\pi}{8}}\frac{\mu}{1-\eta_1}\frac{1}{L(v)}a \\ COD &= a\sqrt{r} \end{aligned} \tag{8}$$

where $K_I(v)$ is dynamic stress intensity factor, $v$ is crack speed, $\mu$ is the modulus of rigidity, $a$ is a proportional constant determined by the COD measurement. The constant $\eta_1$ is equal to $\eta/(1+\eta)$ under the plane stress condition, where $\eta$ is the Poisson's ratio. Functions $A_I(v)$ and $L(v)$ are the functions of crack speed $v$, described as follows,

$$\begin{aligned} A_I(v) &= \frac{\alpha_1(1-\alpha_2^2)}{4\alpha_1\alpha_2-(1+\alpha_2^2)^2} \\ L(v) &= \frac{2\alpha_1(\alpha_1^2-\alpha_2^2)}{4\alpha_1\alpha_2-(1+\alpha_2^2)^2} \\ \alpha_1 &= \sqrt{1-(v/c_1)^2} \\ \alpha_2 &= \sqrt{1-(v/c_2)^2} \end{aligned} \tag{9}$$

where $c_1$ and $c_2$ are the longitudinal and shear wave speed, respectively. Through the above procedure, one can obtain the energy release rate of a crack before bifurcation.

#### 2.5.2 Energy release rate after bifurcation

If the lengths of the two branch cracks are exactly the same and if bifurcation angle $\theta$ tends to zero, the two tips of the branch cracks exist at the same position as the nominal tip of mother crack. Under the circumstances, the two branch

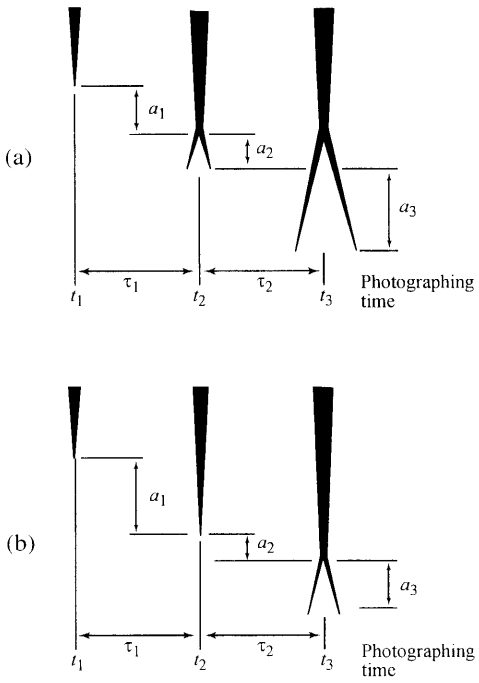


Fig. 5 Crack speed measurement

cracks can be regarded as a single crack, and the COD of mother crack is proportional to the distance $r$ from the nominal tip of the mother crack.

Through the above consideration, it is expected that the COD of mother crack is approximately proportional to $\sqrt{r}$ if the following conditions are satisfied.

( 1 ) Bifurcation angle is small.

( 2 ) The lengths of the two branch cracks are approximately the same.

( 3 ) The lengths of two branch cracks are much smaller than the length of mother crack.

( 4 ) As the result of the above three conditions, the distance between the two branch crack tips are much smaller than the length of the crack.

Experiments with stationary bifurcated notches were carried out and confirmed that the COD of a mother crack is proportional to $\sqrt{r}$ under the above mentioned conditions[19].

If COD of the mother crack is proportional to $\sqrt{r}$ under the above conditions, it is possible to obtain the energy release rate $G(v)$ from the COD measurement of the mother crack. And the energy release rate obtained from the COD measurement of mother crack is thought to be the sum of the energy release rate of the two branch cracks, because the bifurcated crack can be regarded as a single crack under the circumstances that the bifurcation angle is very small. In the present study, energy release rate of a crack after bifurcation is obtained from the COD measurement of mother cracks with Eqs. (8) and (9). The crack speed $v_2$ of the nominal tip of the mother crack is used for the calculation.

**2.5.3 Energy flux** The energy flux $F(v)$ toward a crack tip is given by the product of energy release rate $G(v)$ and crack speed $v$ as follows.

$$F(v) = G(v) \cdot v \tag{10}$$

## 3. Results

The present study measured crack opening displacement, crack speed and energy release rate of eight bifurcating cracks. An example of the eight cracks is shown in the followings.

### 3.1 Specimen after fracture

Figure 6 (a) shows a specimen after fracture. The crack arose at point A on the top boundary of the specimen, propagated downward and bifurcated into two cracks at point BF.

Figure 6 (b) is the magnified photograph around the bifurcation point BF. The crack bifurcated first at point B into Crack 1 and Crack 2, then, Crack 3 bifurcated from Crack 2 at point C. When the holographic recording was taken place Crack 1 was propagating, but it arrested later at point D. In the figure, also shown are the crack tip positions at the holographic recordings of the crack. The crack tip was at 3.1 mm above bifurcation point B at the recording of the first frame. At the recording of the second frame crack tips were at 0.6 mm below point B, and were at 3.4 mm below point B at the recording of the third frame.

### 3.2 Crack at bifurcation

Figure 7 shows the three successive microscopic photographs at the bifurcation of the fast propagating crack shown in Fig. 6. Figure 7 (a), (b) and (c) are the first, the second and the third frames. The time interval $\tau_1$ between the first and the second frame is 5.5 μs and, $\tau_2$ between the second and the third is 4.5 μs. The photographs are so clear that the crack opening displacement can be measured accurately along the crack. Bifurcation angle $\theta$ of the crack is about 14 degrees.

It must be noted that the length of the two branch cracks are the same in Fig. 7 (b) and (c). This fact means that the two branch cracks were propagating at the same speed. The speed of the crack in Fig. 7 was 682 m/s before bifurcation, and 612 m/s after bifurcation. The first frame

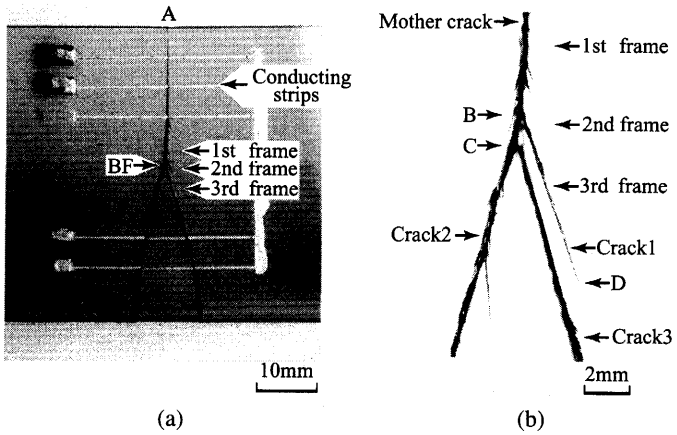


Fig. 6 (a) Specimen after fracture (b) Enlarged picture around the bifurcation point

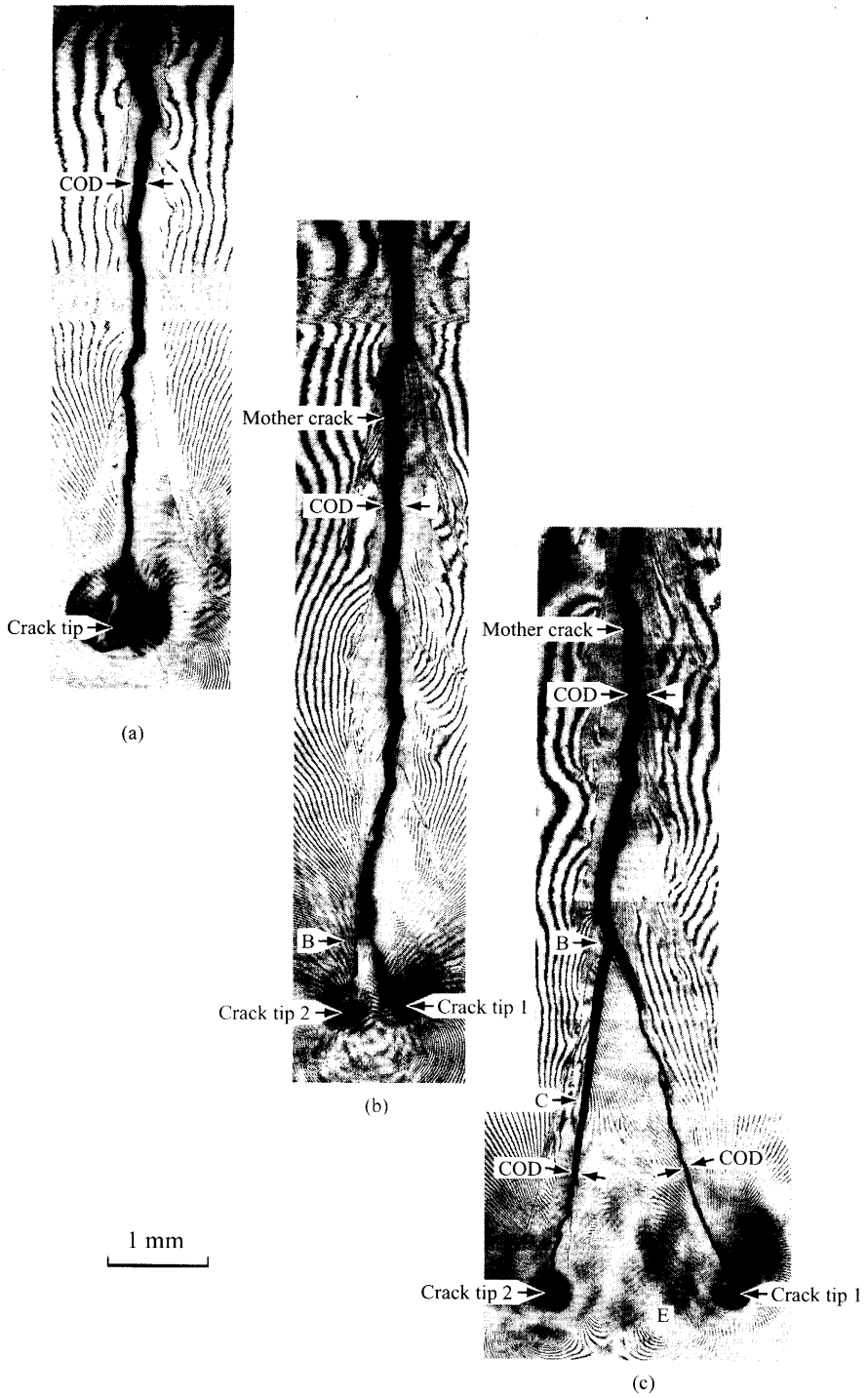


Fig. 7 Microscopic photographs of rapidly bifurcating crack

was photographed at 4.5 μs before bifurcation, the second frame, at 1.0 μs after bifurcation, and the third, at 5.5 μs after bifurcation, respectively.

Figure 6(b) shows that Crack 3 had already bifurcated from Crack 2 at point C before the third frame was recorded. But Crack 3 does not exist in Fig. 7(c). This fact indicates that Crack 3 started bifurcation from Crack 2 in the inside of the specimen or on the specimen surface opposite the photographed surface, but that Crack 3 didn't arrived at the photographed surface yet when the third frame was recorded. Accordingly, it can be said that the rapid crack bifurcation is not two-dimensional but three-dimensional phenomena[1]. This will be discussed later.

Around the crack there are many interference fringes that are created by the interference between the light beam reflected by surface SA and that reflected by surface SB of the specimen. The interference fringes represent the equi-

thickness lines of the specimen or the contours of the sum of principal stresses. It is possible to measure the stress field around the crack tip by analyzing the interference fringes. But the present study focuses the attention mainly onto the COD of the cracks.

### 3.3 Crack opening displacement

Figure 8 (a), (b) and (c) show the results of the COD measurement of the crack in Fig. 7 (a), (b) and (c), respectively. The horizontal axis indicates the distance $r$ from a crack tip, and the vertical scale denotes COD. In the present study, the CODs were measured along cracks from the crack tips up to about 10 mm.

Figure 8 (a) shows the result of COD measurement of a crack before bifurcation. The measurement result says that the COD of the crack before bifurcation is proportional to the square root of the distance $r$ from the crack tip. This result is in agreement with the theoretical and experimental results on fast propagating cracks that are not bifurcated[15),(16),(18)].

On the other hand, shown in Fig. 8 (b) and (c) are the results of COD measurement after bifurcation. The important fact is that, both in Fig. 8 (b) and (c), the COD of the mother crack is proportional to $\sqrt{r}$. It is confirmed that, not only on the crack in Fig. 7 but also on all of the other cracks, the CODs of mother cracks were proportional to the square root of the distance $r$ from the nominal tips of mother cracks which are defined in section 2.3.

But, the CODs of the two branch cracks are not necessarily proportional to $\sqrt{r}$ as shown in Fig. 8 (b) and (c). This may be caused by the three dimensional structure of bifurcating crack tips mentioned in the previous section.

### 3.4 Crack speed

Figure 9 represents the result of crack speed measurement. The vertical axis is the crack speed, and the horizontal axis is the crack tip position measured from the bifurcation point. The negative value of the crack tip position means the cracks before bifurcation, and the positive value means the cracks after bifurcation.

The measurement result clearly shows that there is no discontinuous change of crack speed at the bifurcation point. The mean value of crack speed $v_1$ before bifurcation is $688 \pm 45$ m/s, while the mean of crack speed $v_2$ of the cracks after bifurcation whose tips are within 5 mm from the bifurcation point is $647 \pm 35$ m/s. The mean value of bifurcation angle $\theta$ is 15 degrees in the present study. Thus the mean value of crack speed $v_b$ of branch cracks is $669 \pm 36$ m/s, which is obtained through Eq. (7). Hence it can be said that (1) Crack speed $v_2$ of the nominal tip of the mother crack after bifurcation is smaller than that before bifurcation by 42 m/s, and (2) Crack speed $v_b$ of branch cracks is slower than crack speed $v_1$ before bifurcation by 19 m/s. However the scattering of speed measurement data is from $\pm 35$ to $\pm 45$ m/s. Thus it must be noted that the crack speed change at bifurcation is as small as the scattering of measurement data in the present study.

### 3.5 Energy release rate and energy flux

The COD measurement says that the COD of a crack before bifurcation is proportional to $\sqrt{r}$, and, after bifurcation, the COD of mother crack is proportional to $\sqrt{r}$. Therefore it is possible to obtain the energy release rate $G(v)$ of a crack both before and after bifurcation. Figure 10

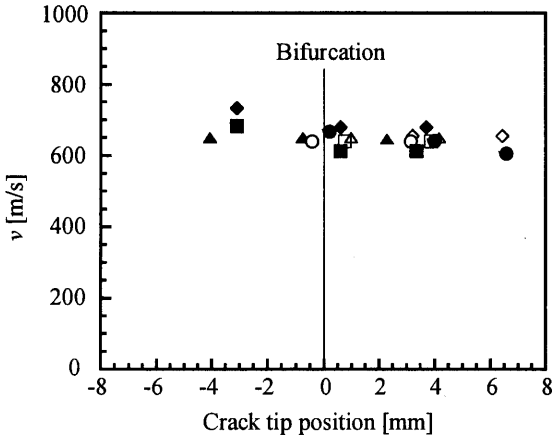


Fig. 9 Crack speed near the bifurcation point

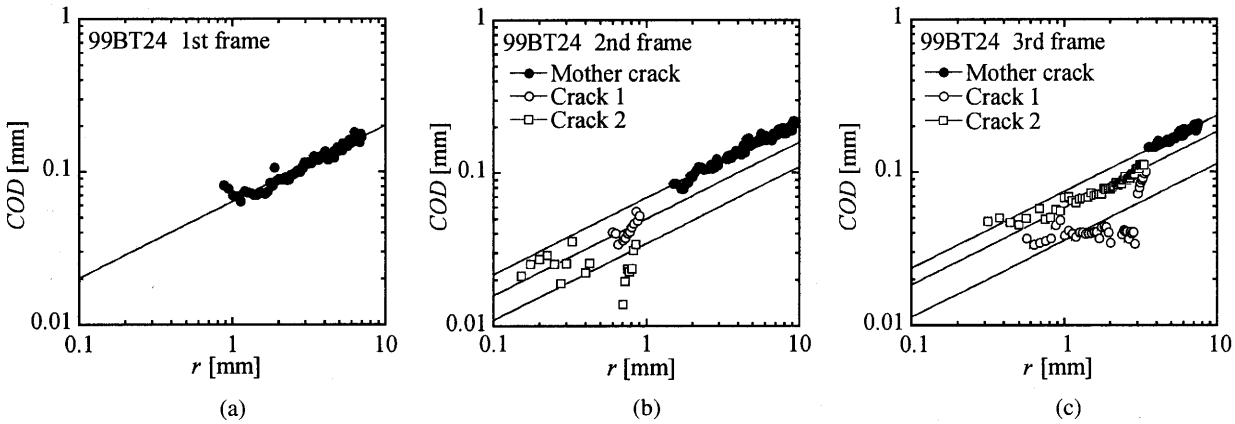


Fig. 8 COD versus $r$

shows the energy release rate just before and after bifurcation. The horizontal axis is the distance measured from the bifurcation point, and the vertical axis is the energy release rate obtained from the COD measurement. It must be noted that there exist no discontinuity of energy release rate. The energy release rate is continuous at the bifurcation point, and increases gradually with crack extension.

Figure 11 shows the energy flux to crack tips. The horizontal scale is the time $t$ measured from the instant of bifurcation, and the vertical scale is the energy flux $F(v)$ that is given by the product of energy release rate and crack speed. The graph says that the energy flux to crack tips is also continuous at the moment of bifurcation. There is no discontinuity of energy flux. This is because there is no discontinuous change both in crack speed and in energy release rate.

## 4. Discussions

### 4.1 Energy release rate given by the COD of mother crack

Energy release rate given by the COD measurement is valid for the cracks before bifurcation, because the CODs are proportional to $\sqrt{r}$ which is in agreement with the theory of dynamic fracture mechanics.

In the case of cracks after bifurcation, the CODs of mother cracks are proportional to the square root of the distance $r$ from the nominal tip of the mother crack, as shown in Fig. 8. This is probably caused by the small bifurcation angle of 15 degrees. Accordingly it can be said that the energy release rate obtained from the COD measurement of mother cracks is valid just after bifurcation where the length of branch cracks are much smaller than the length of the mother crack.

In the case of cracks with longer branch cracks, the energy release rate given by the COD measurement of mother cracks may deviate from the true value of energy release rate. However, the result that the energy release rate is continuous at bifurcation is valid, because the COD measurement of mother cracks gives the correct values of energy release rate just after bifurcation.

### 4.2 Continuity of crack speed and energy release rate

As shown in Figs. 10 and 11, energy release rate and energy flux are continuous at the moment of bifurcation, and don't show discontinuous change within the accuracy of measurement. And the crack speed change at bifurcation is as small as the scattering of measurement data. These facts seem to be difficult to understand on the assumption that the crack bifurcation is two-dimensional phenomena, because crack surfaces increase discontinuously at the moment of bifurcation on the two-dimensional assumption.

As described in section 3.2 and 3.3, the microscopic photographs of bifurcating cracks strongly indicates that the bifurcation process is three-dimensional phenomena[1]. If the bifurcation process is three-dimensional, the fracture surface can increase continuously. As the result, the energy release rate can increase gradually and continuously at the bifurcation point without discontinuous decrease of crack speed.

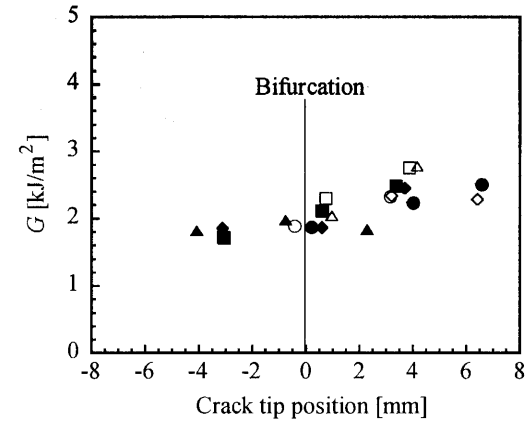


Fig. 10 Energy release rate near the bifurcation point

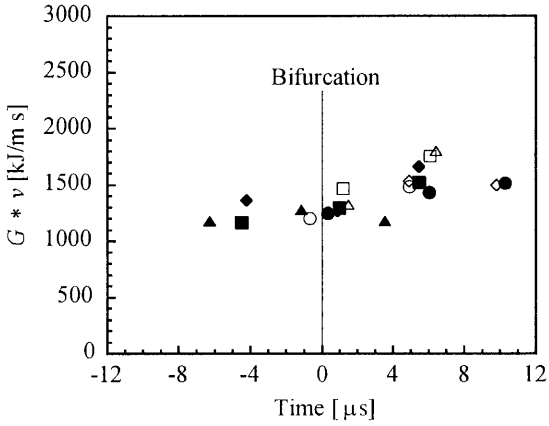


Fig. 11 Energy flux just before and after bifurcation

Figures 9, 10 and 11 shows that the energy release rate and energy flux increases gradually with crack extension even though the crack speed does not increase. This is probably caused by the gradual increase of the area of fracture surfaces during the bifurcation process.

### 4.3 Validity of nominal tip position of mother crack

When the nominal tip position of a mother crack was determined in section 2.3, the branch cracks were thought to be two-dimensional through cracks. But the real branch cracks just after bifurcation are not necessarily two-dimensional through cracks, but often three-dimensional ones as shown in Fig. 7. The present study applied the method to determine the nominal tip positions of mother cracks to all the bifurcated cracks even in the case that branch cracks are likely to have three-dimensional structure. As a result, it was found that the COD of mother cracks is proportional to the distance $r$ from the nominal

tips determined by the method described in section 2.3. The result indicates that the method in section 2.3 is valid to determine the nominal tip position of a mother crack even if the branch cracks have three-dimensional structure. This is probably explained by the following reasons.

The first is that the bifurcation angle is small and bifurcation is approximately symmetric to the direction of the mother crack. It is thus a good assumption that the nominal tip of a mother crack is on the line extrapolated from the mother crack.

The second reason is that all the branch cracks propagates at the same speed. In Fig. 7, the tip of Crack 3 is thought to be at point E between Crack tip 1 and Crack tip 2, because the interference fringes show the stress concentration at point E. This fact says that the tips of Crack 1, 2 and 3 were approximately at the same position in $x$-direction. Consequently, the nominal tip position of the mother crack determined from Crack tip 1 and Crack tip 2 is nearly equal to that determined from the positions of Crack tip 1, 2 and 3.

Through the above examination, it can be said that the three-dimensional structure of bifurcating crack tip doesn't largely affect the position of the nominal tip of a mother crack. The above mentioned is strongly supported by the simultaneous photographing of fast propagating cracks on the both surfaces of specimens done by the authors[20].

## 5. Conclusions

( 1 ) Crack opening displacement (COD) of a fast propagating crack before bifurcation is proportional to the square root of the distance $r$ from the crack tip. After bifurcation, the COD of the mother crack is proportional to $\sqrt{r}$.

( 2 ) Crack speed does not decrease discontinuously at the moment of rapid crack bifurcation.

( 3 ) The energy release rate obtained from the COD measurement increases continuously and gradually at the bifurcation point, and does not show discontinuous increase.

( 4 ) Energy flux is also continuous at the instant of bifurcation. It increases continuously and gradually with crack extension.

## References


( 1 ) Ravi-Chandar, K. and Knauss, W.G., An Experimental Investigation into Dynamic Fracture: III. On Steady-State Crack Propagation and Crack Branching, Int. J. Fracture, Vol.26 (1984), pp.141–154.

( 2 ) Ramulu, M. and Kobayashi, A.S., Mechanics of Crack Curving and Branching — A Dynamic Fracture Analysis, Int. J. Fracture, Vol.27 (1985), pp.187–201.

( 3 ) Yoffe, E.H., The Moving Griffith Crack, Phil. Mag., Vol.42 (1951), pp.739–751.

( 4 ) Baker, B.R., Dynamic Stresses Created by a Moving Crack, Trans. ASME, J. Appl. Mech., Vol.29 (1962), pp.449–458.

( 5 ) Kobayashi, A.S., Wade, B.G., Bradley, W.B. and Chiu, S.T., Crack Branching in Homalite-100 Sheets, Eng. Fract. Mech., Vol.6 (1974), pp.81–92.

( 6 ) Irwin, G.R., Dally, J.W., Kobayashi, T., Fourney, W.L., Etheridge, M.J. and Rossmanith, H.P., On the Determination of the a–K Relationship for Birefringent Polymers, Exp. Mech., Vol.19 (1979) pp.121–128.

( 7 ) Arakawa, K. and Takahashi, K., Branching of a Fast Crack in Polymers, Int. J. Fract., Vol.48 (1991), pp.245–254.

( 8 ) Theocaris, P.S. and Georgiadis, H.G., Bifurcation Predictions for Moving Cracks by the $T$-Criterion, Int. J. Fract., Vol.29 (1985), pp.181–190.

( 9 ) Nishioka, T., Kishimoto, T., Ono, Y. and Sakaura. K., Basic Studies on the Governing Criterion for Dynamic Crack Branching Phenomena, Trans. Jap. Soc. Mech. Eng., (in Japanese), Vol.65, No.633, A (1999), pp.1123–1131.

(10) Suzuki, S., Inayama, A. and Arai, N., Reflection Type High-Speed Holographic Microscopy to Photograph Crack Bifurcation, Experimental Mechanics, Advances in Design, Testing and Analysis, Proc. 11th Int. Conf. on Experimental Mechanics, Vol.1, (1998), pp.583–588, A.A.Balkema, Rotterdam.

(11) Suzuki, S., Inayama, A., Arai, N. and Mizuta, T., Stress Field Measurement at Bifurcation of Fast Propagating Cracks by High-Speed Interferometry, IUTAM Symposium on Advanced Optical Methods and Applications in Solid Mechanics, (2000), pp.587–594, Kluwer Academic Publishers.

(12) Suzuki, S., Sakaue, K., Morita, Y. and Mori, T., Method for Successive Photographing of Rapid Crack Bifurcation by Means of High-Speed Holographic Microscopy, 24th Int. Cong. on High-Speed Photography and Photonics, SPIE, Vol.4182 (2001), pp.480–487.

(13) Suzuki, S., Nozaki, Y. and Kimura, H., High-Speed Holographic Microscopy for Fast-Propagating Cracks in Transparent Materials, Applied Optics, Vol.36 (1997), pp.7224–7233.

(14) Suzuki, S., Kanahashi, Y. and Nakagami, R., Application of High-Speed Holographic Microscopy to Study on Rapid Crack Propagation, 22nd Int. Cong. on High-Speed Photography and Photonics, SPIE, Vol.2869 (1997), pp.644–650.

(15) Suzuki. S., A Method of Pulsed Holographic Microscopy to Photograph Fast Propagating Cracks with Higher Spatial Resolution, Post Conf. Proc. of the 1996 VIII Int. Cong. on Exp. Mech., Society of Exp. Mech., (1996), pp.229–236.

(16) Suzuki, S., Homma, H. and Kusaka, R., Pulsed Holographic Microscopy as a Measurement Method of Dynamic Fracture Toughness for Fast Propagating Cracks, J. Mech. Phys. Solids, Vol.36, No.6 (1988), pp.631–653.

(17) Champagne, E.B., Nonparaxial Imaging, Magnification, and Aberration Properties in Holography, J. Opt. Soc. America, Vol.57, No.1 (1967), pp.51–55.

(18) Freund, L.B., Dynamic Fracture Mechanics, (1990),

pp.160–169, Cambridge Univ. Press.

(19) Suzuki, S., Morita, Y. and Sakaue, K., Measurement of Opening Displacement of Bifurcated Cracks by High-Speed Holographic Microscopy and Moiré Interferometry, Trans. Japan Soc. Mech. Engineers, (in Japanese), Vol.67, No.655, A (2001), pp.432–439.

(20) Suzuki, S. and Sakaue, K., Simultaneous Photographing of Fast Propagating Cracks at Bifurcation on Both Surfaces of Plate Specimens, Trans. Japan Soc. Mech. Engineers, (in Japanese), Vol.68, No.675, A (2002), pp.1674–1680.